

Systematics of  $(\vec{p}, d)$  analyzing powers at 94 MeVH. Nann, D. W. Miller, W. W. Jacobs, D. W. Devins,\* W. P. Jones,  
and Li Qing-Li†

Physics Department, Indiana University, Bloomington, Indiana 47405

(Received 29 October 1982)

Analyzing-power angular distributions of the  $(\vec{p}, d)$  reaction on  $^{60}\text{Ni}$ ,  $^{86}\text{Sr}$ , and  $^{208}\text{Pb}$  have been measured at 94-MeV bombarding energy. A distinctive  $j$  dependence was observed for the pickup of neutrons from the  $p_{1/2}$ ,  $p_{3/2}$ ,  $f_{5/2}$ , and  $f_{7/2}$  orbitals which is independent of target mass and of the number of nodes in the neutron bound-state radial wave function. These characteristic  $j=l\pm\frac{1}{2}$  signatures may thus be used as experimental templates for reliable spin determinations over the whole periodic table at this bombarding energy. Conventional distorted-wave Born approximation calculations using standard optical model parameters describe the experimental analyzing power angular distributions and the associated  $j$  dependence rather poorly.

[ NUCLEAR REACTIONS  $^{60}\text{Ni}$ ,  $^{86}\text{Sr}$ ,  $^{208}\text{Pb}(\vec{p}, d)$ ,  $E=94$  MeV; measured  $A_y(\theta)$ . Enriched targets. DWBA analysis.]

## I. INTRODUCTION

During the past few years, several investigations of deeply-bound neutron hole states using the  $(p, d)$  reaction at bombarding energies near 90 MeV have been reported.<sup>1-3</sup> In these studies, the transferred orbital angular momenta  $l$  were determined from the shape of the differential cross sections; in two cases,<sup>2,3</sup> the transferred total angular momenta  $j$  were obtained from measurements of analyzing-power angular distributions  $A_y(\theta)$ . The method used in Ref. 2 to determine  $j$  for a broad deeply-bound hole state observed in the  $^{120}\text{Sn}(\vec{p}, d)^{119}\text{Sn}$  reaction at 5 MeV excitation was to compare  $A_y(\theta)$  for this transition to the experimental analyzing power pattern of the  $^{90}\text{Zr}(\vec{p}, d)^{89}\text{Zr}$  ground state transition ( $j=\frac{9}{2}$ ). This identification procedure relies on the premise that the  $j$ -dependent features of  $A_y(\theta)$  do not change substantially with target mass. However, prior to the present investigation, little experimental evidence had been reported at this bombarding energy to support this view.

It has also been shown recently<sup>4</sup> that conventional distorted-wave Born approximation (DWBA) calculations at these same energies fail to reproduce experimental analyzing-power angular distributions for transitions to well-known low-lying states [e.g., in the case of the  $^{24}\text{Mg}(\vec{p}, d)^{23}\text{Mg}$  reaction]. Therefore, the use of standard DWBA predictions in order to determine the transferred total angular

momentum from a comparison with experimental  $A_y(\theta)$ 's appears to be quite unreliable. If, however, stable  $j$ -dependent angular patterns of *measured* analyzing powers could be established over the whole periodic table, or at least a large portion of it, these signatures would then make possible reliable spin determinations for neutron hole states independent of DWBA analyses. Moreover, such an experimental result would give a solid justification of the method used, for example, in Ref. 2.

The present measurements of  $(\vec{p}, d)$  analyzing powers at  $E_p=94$  MeV for three targets in the mass range from  $^{60}\text{Ni}$  to  $^{208}\text{Pb}$  were undertaken in order to search for such empirical,  $j$ -dependent  $A_y(\theta)$  signatures and to investigate their stability versus the target mass. Previous results<sup>3</sup> from the  $^{24}\text{Mg}(\vec{p}, d)^{23}\text{Mg}$  reaction at the same bombarding energy were included in this survey. In particular, transitions in which the neutron is picked up from the  $1p$ ,  $2p$ ,  $3p$ ,  $1f$ , and  $2f$  orbitals have been investigated, and the results are reported in Secs. II and III of this paper. In addition, a series of DWBA calculations was performed in an attempt to describe the measured analyzing power angular distributions, as discussed in Sec. IV.

II. EXPERIMENTAL PROCEDURES  
AND RESULTS

A 94-MeV polarized proton beam from the Indiana University Cyclotron Facility was used to per-

form the present measurements. The targets were isotopically enriched, self-supporting  $^{60}\text{Ni}$  (99.8%),  $^{86}\text{Sr}$  (96.9%), and  $^{208}\text{Pb}$  (98.7%) metallic foils of nominal thicknesses 3.3, 4.0, and 3.2 mg/cm<sup>2</sup>, respectively. The reaction products were momentum analyzed in the quadrupole-dipole-dipole-multipole magnetic spectrometer and detected in the focal plane by a position-sensitive helical proportional counter followed by two plastic scintillators. Energy loss  $\Delta E$  signals from the two scintillators were used for particle identification. A more extensive description of the experimental setup can be found elsewhere.<sup>1</sup>

The beam polarization was measured with a  $^4\text{He}$  polarimeter periodically inserted into the beam between the two cyclotrons. The polarization in both "spin up" and "spin down" orientations was monitored and found to vary between 70% and 75%. During data acquisition, the spin direction was automatically flipped every minute in the atomic-beam source. This procedure did not affect the beam intensity or transmission and helped to reduce possible systematic errors in the extracted  $A_y(\theta)$  associated with any slow change in the beam characteristics on target. Further details are given in Ref. 3.

Spectra were taken over the angular range from  $6^\circ$  to  $20^\circ$  in  $2^\circ$  steps, from  $20^\circ$  to  $30^\circ$  in  $2.5^\circ$  steps, and from  $30^\circ$  to  $45^\circ$  in  $3^\circ$  steps. The energy resolution obtained was about 55 keV FWHM. Analyzing-power angular distributions for some typical  $l=1$  and  $l=3$  transitions are shown in Figs. 1 and 2, respectively. In each case the spin of the residual state is well known. Included in Fig. 1 are also the results for  $1p_{1/2}$  and  $1p_{3/2}$  neutron pickup obtained in an earlier study of the  $^{24}\text{Mg}(\bar{p},d)^{23}\text{Mg}$  reaction.<sup>3</sup> It is clear from both figures that, at the more forward angles, very pronounced oscillatory patterns for  $A_y(\theta)$  are observed which demonstrate a clear differentiation between the spin-orbit partners ( $j=l\pm\frac{1}{2}$ ) for all final nuclei in this study. Furthermore, no large variations in the gross features of this  $j$  dependence with mass number are evident at this bombarding energy.

### III. DISCUSSION OF EXPERIMENTAL RESULTS

Results for the  $l=1$  transitions, where the neutron is picked up from the  $p_{1/2}$  and  $p_{3/2}$  orbitals, are shown in Fig. 1. The most characteristic pattern of the analyzing-power angular distribution for the pickup of a  $p_{1/2}$  neutron, shown in the left half of Fig. 1, is the pronounced negative value observed at the very forward angles. In this angular region, the  $A_y(\theta)$  for a  $p_{3/2}$  pickup, shown in the right half of Fig. 1, are close to zero, except for  $^{207}\text{Pb}$ , where

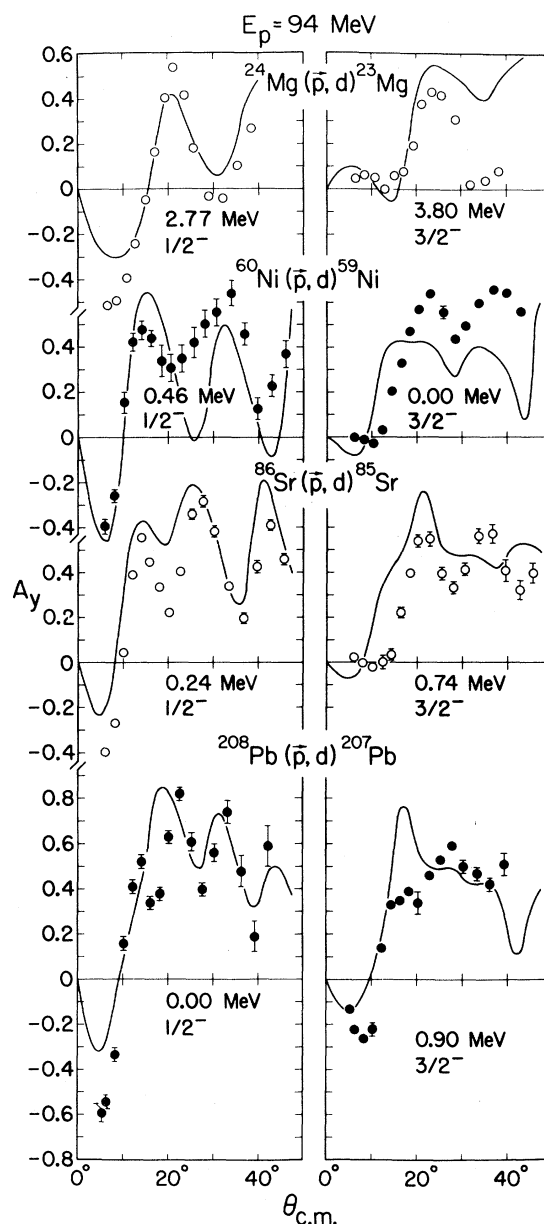


FIG. 1. Analyzing-power angular distributions for  $l=1$  transitions.

small (compared to the corresponding spin-orbit partner) negative values are observed near  $10^\circ$ . The latter deviation from the pattern observed for lower mass targets may result from the higher energy of the outgoing deuterons, since the  $Q$  value for the  $^{208}\text{Pb}(\bar{p},d)^{207}\text{Pb}$  reaction is at least 5 MeV less negative than for the other targets. We observe this forward angle signature of  $A_y(\theta)$  for pickup from  $p_{1/2}$  vs  $p_{3/2}$  orbitals to be stable despite the fact that the number of nodes in the neutron bound-state ra-

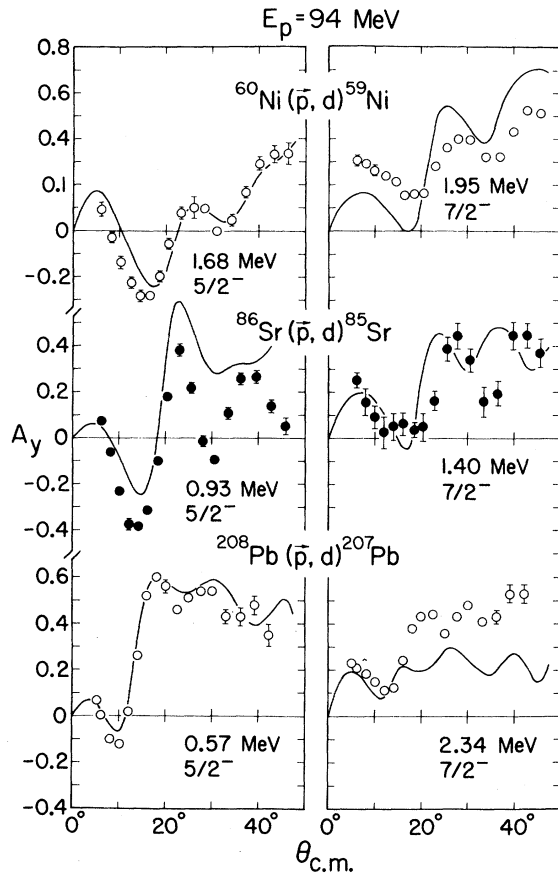


FIG. 2. Analyzing-power angular distributions for  $l=3$  transitions.

dial wave function ranges from 1 for  $^{24}\text{Mg}$  to 3 for  $^{208}\text{Pb}$ . At angles larger than about  $20^\circ$ , the observed analyzing powers for the  $p_{1/2}$  and  $p_{3/2}$  pickup tend to oscillate in an opposite manner (with the exception of  $^{24}\text{Mg}$ ), the minima of the  $p_{1/2}$  analyzing powers coinciding roughly in angle with the maxima of the  $p_{3/2}$  analyzing powers.

For the  $l=3$  transitions, shown in Fig. 2, the neutron is picked up from the  $1f$  ( $^{60}\text{Ni}$  and  $^{86}\text{Sr}$ ) and  $2f$  orbitals ( $^{208}\text{Pb}$ ). Again, one very characteristic  $j$ -dependent feature which is independent of the target mass and number of radial nodes was observed. The signature of the  $f_{5/2}$  pickup is the negative lobe in  $A_y(\theta)$  around  $10^\circ$  to  $15^\circ$ . In this angular region, the analyzing power for an  $f_{7/2}$  pickup is positive. For larger angles, we observe in one case ( $^{60}\text{Ni}$ ) very similar oscillatory behavior for the two  $l=3$  spin-orbit partners, whereas for the other targets the analyzing powers tend to oscillate roughly in an opposite manner, although not as strongly as for the  $l=1$  transitions.

We note that 94 MeV appears to be the highest

bombarding energy at which the analyzing power angular distributions for the  $(\bar{p}, d)$  reaction on heavier mass targets show characteristic  $j$ -dependent features, albeit in a rather restricted angular range. Kraushaar *et al.*<sup>5</sup> observed almost no  $j$  dependence in  $A_y(\theta)$  for neutron hole states studied in the  $^{208}\text{Pb}(\bar{p}, d)^{207}\text{Pb}$  reaction at 123-MeV bombarding energy. Our  $(\bar{p}, d)$  analyzing power distributions for this target at 94 MeV bombarding energy show the general  $j$ -dependent signatures as described above, but they are less distinct than those for the lighter targets.

In summary, the present analyzing power angular distributions at  $E_p=94$  MeV show characteristic  $j$ -dependent features for  $l=1$  and  $l=3$  transfer which at angles below  $15^\circ$  to  $20^\circ$  are independent of the target mass over the range  $A=24$  to 208. The small observed shifts of the maxima and minima to smaller angles (for both the  $l=1$  and  $l=3$  transitions) as a function of increasing target mass can be explained kinematically, resulting from changes in the transferred momenta and interaction radii.

The present conclusions at 94 MeV are different from those obtained at lower energies by Hosono *et al.*,<sup>6</sup> who studied analyzing power angular distributions of the  $(\bar{p}, d)$  reaction at 65 MeV on several target nuclei ranging from  $^{12}\text{C}$  to  $^{94}\text{Zr}$ . On the basis of the oscillatory pattern and the position of the maxima and minima, these authors were able to categorize their  $A_y(\theta)$  according to the number of nodes  $n$  of the radial bound state wave function of the transferred neutron with either  $j(n)=l+\frac{1}{2}$  or  $j(n)=l-\frac{1}{2}$ . The only exception observed was the neutron pickup from the  $1p_{1/2}$  orbital, which did not follow the usual  $n=1, j=l-\frac{1}{2}$  pattern. Our results at 94 MeV do not show such an  $n$  dependence, at least for angles below  $20^\circ$ . For angles greater than  $20^\circ$ , in the angular region of mutually overlapping measurements, we also come to different conclusions than that of Ref. 6. Although certain features of the  $n=1$  or 2,  $j_>=l+\frac{1}{2}$  or alternatively  $n=1$  or 2,  $j_<=l-\frac{1}{2}$  distributions bear some resemblance to each other, in general we observe both larger variations in the amplitude of the oscillations and/or significant variations in the oscillatory pattern itself, than was reported at 65 MeV. In short, we observe a  $j$  dependent signature in  $A_y(\theta)$  over a restricted angular region which is independent of  $n$ . DWBA calculations, as discussed later, confirm these experimental observations that at  $E_p=94$  MeV the  $j$ -dependent features of  $A_y(\theta)$  do not depend on the number of radial nodes.

#### IV. DWBA COMPARISONS

It is of interest to compare DWBA predictions to the measured analyzing-power angular distributions

TABLE I. Optical model parameters used in the DWBA calculations.

Target	Particle	$V$ (MeV)	$r_0, a$ (fm)	$W_v$ (MeV)	$4W_s$ (MeV)	$r', a'$ (fm)	$V_{so}$ (MeV)	$W_{so}$ (MeV)	$r_{so}, a_{so}$ (fm)	$r_c$ (fm)
$^{24}\text{Mg}$	$p$	27.1	1.25, 0.75	8.9		1.40, 0.55	5.75	3.4	1.08, 0.66	1.25
	$d$	71.8	1.25, 0.75		94.0	1.25, 0.75	3.60		1.25, 0.75	1.30
$^{60}\text{Ni}$	$p$	28.2	1.25, 0.75	8.9		1.40, 0.55	6.00	3.4	1.08, 0.66	1.25
	$d$	73.9	1.25, 0.75		94.0	1.25, 0.75	3.60		1.25, 0.75	1.30
$^{86}\text{Sr}$	$p$	28.0	1.25, 0.75	8.0		1.40, 0.55	6.18	3.4	1.08, 0.66	1.25
	$d$	75.1	1.25, 0.75		94.0	1.25, 0.75	5.20		1.25, 0.75	1.30
$^{208}\text{Pb}$	$p$	30.6	1.25, 0.75	8.9		1.40, 0.55	6.68	3.4	1.08, 0.66	1.25
	$d$	79.9	1.25, 0.75		94.0	1.25, 0.75	5.80		1.25, 0.66	1.30
	bound state		1.25, 0.75					$\lambda=25$		

for the  $l=1$  and  $l=3$  transitions. Such a comparison is not only useful from the reaction mechanism point of view, but also may serve as an additional check of the experimentally determined  $j$ -dependent templates and/or reliability of DWBA-generated  $j$ -dependent features. Conventional DWBA calculations were performed using the code DWUCK,<sup>7</sup> and using proton<sup>8</sup> and deuteron<sup>9</sup> optical parameters from the literature. The standard nonlocality parameters of 0.85 and 0.54 fm were used for the proton/neutron and deuteron channels, respectively. A finite-range correction parameter of 0.621 was employed.

With these parameters, the agreement between the calculation and measured  $A_y(\theta)$  was poor, especially at angles below  $20^\circ$ , where the DWBA is expected to be best justified and the strong  $j$  dependence of  $A_y(\theta)$  is observed experimentally. Better agreement was obtained by arbitrarily increasing the depth of the imaginary potential of the deuteron channel. These parameters are given in Table I and the calculated results are shown by the solid lines in Figs. 1 and 2. With this altered parameter set, the agreement with the experimental data is quite reasonable. Similarly, the shapes of the differential cross sections are also better accounted for, although the improvement is less than for the analyzing powers. The magnitudes of the calculated differential cross sections change up to 40% depending on target nucleus and particular transition. Thus, the reliability of extracting spectroscopic factors is quite reduced and needs to be addressed in more detail.

The effect of increasing the absorption in the deuteron optical potential is to reduce the amplitude of the low partial waves in the nuclear interior. Similar improved agreement with the experimental

data can be achieved by employing a lower radial cutoff in the DWBA calculations. This is consistent with the results reported by Shepard *et al.*,<sup>4</sup> who obtained a much better agreement between DWBA predictions and experimental data<sup>3</sup> for the  $l=0$  transition to the 2.36-MeV,  $j^\pi = \frac{1}{2}^+$  state in the  $^{24}\text{Mg}(\vec{p}, d)^{23}\text{Mg}$  reaction by introducing either a stronger absorption in the deuteron channel, or a lower radial cutoff.

The concept of damping the nuclear interior region in DWBA calculations in order to obtain better agreement with the experimental data is far from new. The effects of such damping, however, are even more conspicuous at 94-MeV bombarding energy than at lower energies, and in addition affect transitions with larger values of the transferred orbital angular momenta. Many physical reasons for the damping and associated procedural remedies have been suggested in the past, such as nonlocality and finite-range corrections,<sup>10</sup> density-dependent corrections of the interaction  $V_{pn}$ ,<sup>11</sup> effects of the  $D$ -state component of the deuteron wave function,<sup>12</sup> or deuteron breakup.<sup>13</sup> However, none of the foregoing suggestions has satisfactorily solved all aspects of the problem so far. Recent distorted-wave calculations based upon the use of the Dirac equation rather than the Schrödinger equation<sup>14</sup> have shown some success in describing  $(\vec{p}, d)$  data at higher energies. These calculations in the Dirac formulation predict a natural damping of the distorted waves in the interior of the nucleus and, therefore, ensure improvement over conventional calculations. It is obviously important to carry out further studies attempting to elucidate the behavior of the distorted waves in the nuclear interior for transitions in this energy region.

## V. CONCLUSIONS

The analyzing powers obtained for the  $(\vec{p},d)$  reaction on  $^{24}\text{Mg}$ ,  $^{60}\text{Ni}$ ,  $^{86}\text{Sr}$ , and  $^{208}\text{Pb}$  at 94 MeV incident energy exhibit a systematic  $j$  dependence which, at very forward angles, is nearly independent of the target mass. The observed characteristic features thus provide experimental templates of  $(\vec{p},d)$  analyzing powers for reliable spin determinations over the whole periodic table. These templates can now be used with confidence at 94-MeV bombarding energy for the determination of spins of deeply-bound hole states, which are of current interest. The results justify the method used in Ref. 2, for example, where it was assumed that the  $j$ -dependent features of  $A_y(\theta)$  do not change with target mass between  $A=90$  and 120. The results obtained at 94-MeV bombarding energy are different from those of an earlier systematic  $(\vec{p},d)$  study<sup>6</sup> at  $E_p=65$  MeV ( $12 \leq A \leq 94$ ), which reported a  $j$

dependence in  $A_y(\theta)$  which was dependent on the number of nodes in the picked-up neutron bound-state radial wave function.

Although some qualitative agreement between DWBA calculations and experimental analyzing-power angular distributions has been achieved (albeit with an *arbitrarily* increased deuteron absorption, effectively causing a damping of the distorted waves in the nuclear interior), the stability of the characteristic experimental pattern provides a much more reliable method for spin determination than the DWBA predictions. The problems at present with the DWBA calculations call for additional investigations, both experimental and theoretical, to provide insight into the transfer reaction mechanisms, possible damping mechanisms for the wave functions, and related topics.

This work was supported in part by the U.S. National Science Foundation.

\*Present address: Koppers Process Technologies, 5600 Oak Brook Parkway, Suite 100, Norcross, GA 30093.

†Permanent address: Institute of Atomic Energy, Academia Sinica, P.O. Box 275, Beijing, China.

<sup>1</sup>D. W. Miller, W. P. Jones, D. W. Devins, R. E. Marrs, and J. Kehayias, Phys. Rev. C **20**, 2008 (1979).

<sup>2</sup>G. M. Crawley, J. Kasagi, S. Gales, E. Gerlic, D. Friesel, and A. Bacher, Phys. Rev. C **23**, 1818 (1981).

<sup>3</sup>D. W. Miller, W. W. Jacobs, D. W. Devins, and W. P. Jones, Phys. Rev. C **26**, 1793 (1982).

<sup>4</sup>J. R. Shepard, E. Rost, and P. D. Kunz, Phys. Rev. C **25**, 1127 (1982).

<sup>5</sup>J. J. Kraushaar, J. R. Shepard, D. W. Miller, W. W. Jacobs, W. P. Jones, and D. W. Devins, Nucl. Phys. (to be published).

<sup>6</sup>K. Hosono *et al.*, Nucl. Phys. **A343**, 234 (1980).

<sup>7</sup>P. D. Kunz, University of Colorado (unpublished).

<sup>8</sup>A. Nadasen *et al.*, Phys. Rev. C **23**, 1023 (1981).

<sup>9</sup>G. Mairle, K. T. Knöpfle, H. Riedesel, G. J. Wagner, V. Bechtold, and L. Friedrich, Nucl. Phys. **A339**, 61 (1980).

<sup>10</sup>P. J. Philpott, W. T. Pinkston, and G. R. Satchler, Nucl. Phys. **A119**, 241 (1968); J. K. Dickens, R. M. Drisko, F. G. Perey, and G. R. Satchler, Phys. Lett. **15**, 337 (1965).

<sup>11</sup>B. M. Freedom, J. L. Snelgrove, and E. Kashy, Phys. Rev. C **1**, 1132 (1970).

<sup>12</sup>E. Rost and J. R. Shepard, Phys. Lett. **59B**, 413 (1975).

<sup>13</sup>G. H. Rawitscher and S. N. Mukherjee, Phys. Lett. **110B**, 189 (1982).

<sup>14</sup>E. Rost, J. R. Shepard, and D. Murdock, Phys. Rev. Lett. **49**, 448 (1982).